Role of α-Synuclein Carboxy-Terminus on Fibril Formation in Vitro†

Ian V. J. Murray,‡ Benoit I. Giasson,‡ Shawn M. Quinn,‡ Vishwanath Koppaka,§ Paul H. Axelsen,§ Harry Ischiropoulos,|| John Q. Trojanowski,‡,⊥ and Virginia M.-Y. Lee*,‡

The Center for Neurodegenerative Disease Research, Department of Pathology and Laboratory Medicine, and Department of Pharmacology, University of Pennsylvania School of Medicine, Philadelphia, Pennsylvania 19104, Stokes Research Institute, Children's Hospital of Philadelphia, Philadelphia, Pennsylvania 19104, and Institute on Aging, University of Pennsylvania, Philadelphia, Pennsylvania 19104

Received December 16, 2002; Revised Manuscript Received May 22, 2003

ABSTRACT: Alpha-synuclein (α-syn) is the major component of intracellular inclusions in several neurodegenerative diseases, and the conversion of soluble α-syn into filamentous aggregates may contribute to disease pathogenesis. Since mechanisms leading to the formation of α-syn inclusions are unclear, in vitro models of α-syn aggregation may yield insights into this process. To that end, we examined the consequences on the progressive deletion of the carboxy-terminus of α-syn in regulating fibril formation, and we show here that carboxy-terminal truncated α-syn proteins aggregate faster than the full-length molecule. Protease digestion and immunoelectron microscopy indicate that the α-syn amino- and carboxy-termini are more solvent exposed than the central core and that filaments formed from carboxy-terminal truncated α-syn are narrower in diameter than the full-length molecule. Moreover, seeding experiments under conditions where full-length α-syn did not readily aggregate revealed that carboxy-truncated α-syn extending from amino acids 1−102 and 1−110 but not 1−120 were efficient in seeding full-length α-syn aggregation over a range of concentrations. Using site-directed mutagenesis, the negatively charged residues 104, 105 and 114, 115 in the carboxy-terminus were implicated in this reduced aggregation and the lack of seeding of full-length α-syn fibrillogenesis by 1−120. Our data support the view that the middle region of α-syn forms the core of α-syn filaments and that negative charges in the carboxy-terminus counteract α-syn aggregation. Thus, the carboxy-terminus of α-syn may regulate aggregation of full-length α-syn and determine the diameter of α-syn filaments.

Alpha-synuclein (α-syn),[1] normally a soluble protein localized primarily at the presynaptic region of axons, occurs as filamentous inclusions known as Lewy bodies (LBs) and Lewy neurites (LNs) in several neurodegenerative diseases known as synucleinopathies that include Parkinson's disease (PD), dementia with LBs (DLB), and LB variant of Alzheimer's disease (LBVAD) (*1*−*3*). A role for α-syn in disease pathogenesis is supported by the identification of the A53T and A30P mutations in the α-*syn* gene of rare familial PD pedigrees (*4*, *5*) and by growing evidence that α-syn is the building block of pathological filaments in LBs and LNs of diverse neurodegenerative synucleinopathies (*1*−*3*). Recent studies have shown that α-syn aggregates can be detected in transgenic mouse models as well as transgenic flies overexpressing α-syn, and the formation of these aggregates causes neurodegeneration and motor impairments in these models (*6*−*10*). Neuronal and oligodendroglia filamentous α-syn pathology also is abundant in multiple system atrophy (MSA) and neurodegeneration with brain iron accumulation type I (NBIA) (*11*−*13*).

The major ultrastructural component of pathological α-syn inclusions are 10−20 nm wide filaments. The finding that recombinant α-syn readily polymerizes into filaments in vitro (*14*−*18*) further supports the notion that α-syn is the building block of these fibrous lesions. Moreover, the fibrils in these pathological inclusions are intensely labeled by antibodies to α-syn in situ (*2*, *3*, *11*, *19*−*21*), and partially purified filaments from PD, DLB, and MSA brains are decorated with anti-α-syn antibodies (*12*, *21*, *22*).

Several reports have defined a number of the chemical conditions, molecular interactions, and possible intermediates involved in the fibrillization of α-syn (*14*−*17*, *23*−*35*). In vitro aggregation of α-syn is a nucleation dependent process (i.e., fibril formation displays a lag phase followed by a rapid increase in fibril formation (*17*, *25*, *29*, *36*)). This lag phase is dramatically reduced by the addition of a seed or nucleus of pre-aggregated α-syn (*25*, *30*), and it has been proposed

† This work was funded by grants from the NIA (H.I., J.Q.T., and V.M.-Y.L.) and an Alzheimer's Association Pioneer Award. B.I.G. and I.V.J.M. are recipients of fellowships from the Canadian Institutes of Health Research. P.H.A. is supported by NIH Grants GM54617 and AI43412 and the American Heart Association. V.K. is supported by NIH Grant HL68186 and the American Heart Association.

* Corresponding author. E-mail: vmylee@mail.med.upenn.edu. Tel: (215) 662-6427. Fax: (215) 349-5909.

‡ Department of Pathology and Laboratory Medicine, University of Pennsylvania School of Medicine.

§ Department of Pharmacology, University of Pennsylvania School of Medicine.

|| Children's Hospital of Philadelphia.

⊥ University of Pennsylvania.

[1] Abbreviations: ANS, 8-anilino-1-naphthalenesulphonic acid; CD, circular dichroism; ATR-FTIR, attenuated total internal reflection Fourier transformed infrared spectroscopy; EM, electron microscopy; LB, Lewy bodies; LBVAD, Lewy body variant of Alzheimer's disease; MSA, multiple system atrophy; PD, Parkinson's disease; α-syn, α-synuclein.

10.1021/bi027363r CCC: $25.00
Published on Web 06/25/2003

that α-syn progresses from an unordered monomer through a partially folded intermediate fibril nucleus to finally elongate into mature filaments (*29*).

While the central region (known as NAC) of α-syn is necessary for fibrillization (*23*, *24*, *37*, *38*), other regions may play a role in this process. For example, both α-syn mutations are located in the amino terminus, and the A53T mutant α-syn fibrillizes faster and more efficiently than wild-type α-syn suggesting that this region of α-syn is important for filament formation (*14*, *16*, *17*, *36*, *39*). However, the propensity to fibrillize increases with decreasing pH (*15*, *29*) and with removal of variable lengths of the negatively charged carboxy-terminus (*28*, *40*), thereby implicating this negatively charged domain in regulating α-syn fibrillization.

We have characterized the aggregation properties of recombinant full-length and truncated α-syn proteins utilizing several different physical and biochemical methods. We have also conducted structural and functional studies to investigate a potential mechanism of this aggregation. On the basis of these studies, a model emerges wherein the NAC region forms the core of the fibril, while the amino- and carboxy-terminal regions of α-syn are peripheral. By using a number of truncated α-syns to seed the full-length protein, we demonstrate that aggregation appears to involve the central hydrophobic NAC region that is regulated by the negatively charged carboxy-terminus.

EXPERIMENTAL PROCEDURES

Expression and Purification of α*-Syn.* Full-length and truncated recombinant human α-syn proteins (corresponding to amino acids 1−89, 1−102, 1−110, 1−120, and 1−130 of α-syn) were expressed in *Escherichia coli* BL21 (DE3) using the bacterial expression vector pRK172, where the α-syn cDNA was cloned into the Nde I and Hind III restriction sites (*40*). The constructs expressing the carboxy-terminal truncated α-syn proteins were engineered using the QuikChange site-directed mutagenesis kit (Stratagene, La Jolla, CA). Stop codons were introduced into the wild-type cDNA, using complimentary sets of synthetic single-stranded DNA by polymerase chain reactions as previously described (*23*). The 1−120/E104A−E105A and 1−120/E114A−D115A constructs were created within the 1−120 construct, where the point mutations (E104A, E105A and E114A, D115A) were introduced in a similar fashion as described above. The codons were changed to reflect that of the desired amino acid with the complement primer as follows: 104−105 For C CAG TTG GGC AAG AAT GCA GCA GGA GCC CCA CAG GAA GG and 114−115 For AA CCA CAG GAA GGA ATT CTG GCA GCT ATG CCT GTG G, with the inverse complement not shown. The sequences of the constructs were verified using the T7 primer and an ABI Prism 377 DNA sequencer (PE Biosystems, Foster, CA) as a service provided by the Nucleic Acid/Protein Research Core Facility at the Children's Hospital of Philadelphia.

Following expression and sedimentation, the bacterial pellets from 1 L of TB broth were resuspended in 40 mL of high-salt (HS) buffer (0.75 M NaCl, 50 mM Tris, pH 7.4, 1 mM EDTA) containing a cocktail of protease inhibitors, heated to 100 °C for 10 min, and centrifuged at 20 000*g* for 10 min. The solution was exchanged with the buffers used for ion exchange chromatography without NaCl by dialysis overnight, and the volume of the supernatants was reduced to 2 mL using Centriprep-10 concentrators (Millipore Corp., Bedford, MA). All proteins were separated by size exclusion using a Superdex 200 HR 10/30 gel filtration column (Amersham Pharmacia Biotech, Inc., Piscataway, NJ) with the appropriate buffers without NaCl (see below). The truncated proteins were separated by different ion exchange chromatography, according to their predicted isoelectric points. Full-length α-syn and truncated α-syn proteins extending over amino acids 1−130 and 1−120 were applied onto a Resource Q column (Amersham Pharmacia Biotech, Inc., Piscataway, NJ) and eluted in 10 mM Tris pH 7.5 using a linear gradient of 0−1 M NaCl gradient. The carboxy-terminal truncated α-syn 1−89, 1−102, and 1−110 proteins, which showed higher isoelectric points than full-length α-syn, were separated on a Resource S column (Amersham Pharmacia Biotech, Inc., Piscataway, NJ) using a linear gradient of 0−1 M NaCl in 50 mM MES buffer, pH 6.5 (*40*). The point mutations 1−120/E104A−E105A and 1−120/E114A−D115A, created within α-syn 1−120, were also separated on a Resource S column, however, in 10 mM Tris buffer, pH 8.5 and a linear salt gradient. The protein concentrations were determined using the bicinchoninic acid (BCA) protein assay (Pierce, Rockford, IL) with bovine serum albumin as standard.

Fibril Assembly, Centrifugal Sedimentation, and Turbidity Analysis. In all experiments, except for circular dichroism and ATR-FTIR measurements, α-syn proteins were polymerized by incubation at 37 °C in 100 mM sodium acetate (pH 7.5) at 100 or 350 μM as indicated, with continuous shaking for 1−2 days as in previous reports (*16*, *23*). For co-assembly/seeding experiments, truncated and full-length α-syn were incubated at a total concentration of 200 μM at molar ratios of 5:1, 1:1, and 1:5 for 1 day (i.e., conditions under which full-length α-syn does not aggregate). Centrifugal sedimentation at 100 000*g* for 30 min was used to pellet out polymerized α-syn. SDS-sample buffer (10 mM Tris, pH 6.8, 1 mM EDTA, 40 mM DTT, 1% SDS, and 10% sucrose) was added to the separated pellets and supernatants, which were heated to 100 °C for 10 min. α-syn proteins were resolved by SDS−PAGE, stained with Coomassie Blue R-250, and quantified by densitometry. The data are presented as the percentage of pelleted protein or as a representative Coomassie stained gel. For turbidity experiments, the OD_{400} of the samples was measured on a spectrophotometer (Beckman DU 640, Beckman, Fulerton, CA) as previously described (*23*, *30*).

Antibodies. The polyclonal antibodies SNL1 (epitope 104−119) and the monoclonal antibodies (MAb) Syn 204 (epitope 89−110) and Syn505 (epitope 2−12) were previously described (*41*, *42*). The polyclonal antibodies SNL-4, NAC, and Syn 43−57 were obtained by immunizing rabbits (Covance, Richmond, CA) with synthetic peptides corresponding to amino acids 2−12, 75−91, and 43−57 of α-syn, respectively (HM Keck Institute, Yale), cross-linked to chemically activated BSA and KLH (Pierce, Rockford, IL), and affinity purified against α-syn coupled to Affigel 10 (Pierce).

K114, Thioflavin T, and ANS Fluorometry. K114 [(*trans*,*trans*)-1-bromo-2,5-bis-(4-hydroxy)styrylbenzene], a novel congener of Congo red (*59*), X-34 (*43*), and BSB (*44*), as well as Thioflavin T (ThioT) were used to measure the

amyloidogenicity of α-syn. A fresh stock of 50 μM K114 was prepared in 100 mM glycine, pH 8.5, and 100 μL of this solution was added to 17.5 μL of undiluted α-syn. Fluorescence at 550 nm, with a long pass filter cutoff of 530 nm, was measured after 20 min on a Spectra Max Gemini spectrofluorometer equipped with SoftMax Pro software (Molecular Devices, CA) using an excitation wavelength of 380 nm.

ThioT fluorescence was measured according to previous reports with some modifications (*26*, *27*). A fresh 0.1 M stock solution of ThioT was prepared, filtered through a 0.2 μm cellulose acetate filter, and diluted to 100 μM ThioT in 100 mM glycine, pH 8.5. α-syn was diluted in water to 17.5 μM, in a final volume of 50 μL to which 50 μL of 100 μM ThioT was added. Fluorescence at 490 nm, with a long pass filter cutoff of 475 nm, was measured within 1−2 min on a Spectra Max Gemini spectrofluorometer using an excitation wavelength of 440 nm.

For ANS binding assays, 1 μL of a 20 μM methanolic solution of ANS was added to 100 μL of 8.75 μM α-syn in PBS at pH 7.4 and incubated for 30 min at room temperature. Fluorescence at 490 nm, with a long pass filter cutoff of 475 nm, was measured with the Spectra Max Gemini spectrofluorometer equipped with SoftMax Pro software (Molecular Devices, CA) using an excitation wavelength of 390 nm. Data are shown corrected for baseline ANS fluorescence.

Proteinase K Digestion of Aggregated α-Syn. Proteinase K digestion of aggregated and unaggregated α-syn was performed as described previously (*23*). Briefly, 250 μg of aggregated or unaggregated synuclein, diluted to 2 μg/μL in water, was incubated with 17.5 μg of Proteinase K (Fisher Scientific) in a final volume of 175 μL at 37 °C for 30 min. The digestion was terminated by adding 2 μL of 0.5 M PMSF and boiling immediately in SDS sample buffer for 10 min at 100 °C.

Negative Staining Electron Microscopy. Fibrillized α-syn proteins were adsorbed onto 300 mesh carbon coated copper grids, stained with 1% aqueous uranyl acetate, and visualized with a JEOL 1010 transmission electron microscope (EM) (Peabody, MA). EM images were captured with a Hamamatsu digital camera (Bridgewater, MA) using AMT software (Danvers, MA). For diameter determination, the widths of 100−120 filaments were measured using Image-Pro Plus software (Media Cybernetics, Del Mar, CA).

Immunoelectron Microscopy. Fibrillized α-syn proteins were adsorbed onto 300 mesh carbon coated nickel grids, blocked with 1% bovine serum albumin for 15 min, and immunostained for 30 min with affinity purified antibodies for immuno-EM studies. The filaments were decorated with anti-rabbit or -mouse antibodies conjugated to 5 nm gold particles (AuroProbe EM, Amersham) and negatively stained with 1% aqueous uranyl acetate. Control grids were incubated with secondary antibody alone. The grids were visualized at a magnification of 120 000× with a JEOL 1010 transmission electron microscope. EM images were captured with a Hamamatsu digital camera using AMT software as described.

Far-UV Circular Dichroism (CD) Spectroscopy. α-syn at 2 mg/mL in 100 mM phosphate buffer, pH 7.6, was left unaggregated or aggregated at 37 °C for 2 days with constant shaking. The proteins analyzed by CD were diluted to 0.25 mg/mL in double distilled water and transferred to a 0.1 cm quartz cuvette (Aviv, Lakewood, NJ). Spectra were collected between 180 and 280 nm with an Aviv 62DS spectrophotometer (Aviv). The protein concentration of the sample was determined with the BCA protein assay using BSA as standard (Pierce).

Attenuated Total Internal Reflection Fourier Transform Infrared Spectroscopy (ATR-FTIR). ATR-FTIR spectroscopy was performed using a continuously purged Bio-Rad FTS-60A FTIR spectrometer, unpolarized light, a horizontal 50 × 10 × 2 mm germanium internal reflection crystal with 45° end facets, and a liquid-nitrogen cooled MCT detector. Spectra were collected as 1024 co-added interferograms in rapid-scanning mode with a resolution of 2 cm^{-1}, scanning speed of 20 MHz, triangular apodization, and one level of zero filling. 5 μL samples of aggregated or unaggregated α-syn, at 2 μg/μL in 10 mM HEPES buffer pH 7.4, were applied to the crystal and either air-dried or dried as rapidly as possible under argon. Background spectra were collected immediately before applying sample, and sample spectra were collected as soon as samples appeared to be dry. Spectral amplitudes have been normalized, but no smoothing, water vapor subtraction, nonlevel baseline correction, or deconvolution procedures were performed on the spectra.

RESULTS

Carboxy-Terminal Deletion Increases α-Syn Aggregation. To assess the ability of carboxy-terminal truncated recombinant α-syn proteins to polymerize into fibrils, the mutant α-syn were compared to the full-length protein using previously established conditions for assembly (*16*). Turbidity and centrifugal sedimentation analyses were used to compare the assembly properties of full-length and carboxy-truncated α-syn at 350 and 100 μM. Evaluation of assembly by turbidity at 350 μM demonstrated that 1−110, 1−120, and 1−130 truncated α-syn assembled more readily than the full-length protein consistent with previous findings (*28*) (Figure 1A). The aggregation of the truncations 1−89 and 1−102 is less robust than that of the other three truncations but better than that of full-length α-syn (Figure 1A). We also noted that the pH of the solutions did not change over time for all the α-syn proteins. Reduction in the concentrations used for aggregation from 350 to 100 μM revealed more striking differences (Figure 1B). The 1−89 and 102 were again less robust than 1−110; however, the longer truncations (1−120 and 1−130) and full-length α-syn appeared to assemble less efficiently at 100 μM than at higher concentrations (Figure 1B). This is particularly evident after 24 h of assembly.

Centrifugal sedimentation was used to compare the assembly of the full-length and truncated α-syn proteins, and the data are represented as a percentage of the pelletable α-syn versus the total α-syn quantified after SDS−PAGE (Figure 1E). All of the truncated proteins (i.e., 1−89 through 1−130) aggregated more rapidly than full-length α-syn after 24 h at a concentration of 350 μM (Figure 1C) with about 70−80% of the truncated α-syn recovered in the pellet fraction when compared to about 25% of the full-length protein. However, by 48 h, full-length and truncated α-syn reached maximum assembly. The shorter truncated α-syn proteins (i.e., the 1−89, 1−102, and 1−110 α-syn species) had an even greater propensity to aggregate since only 100 μM of these truncated proteins were required for assembly,

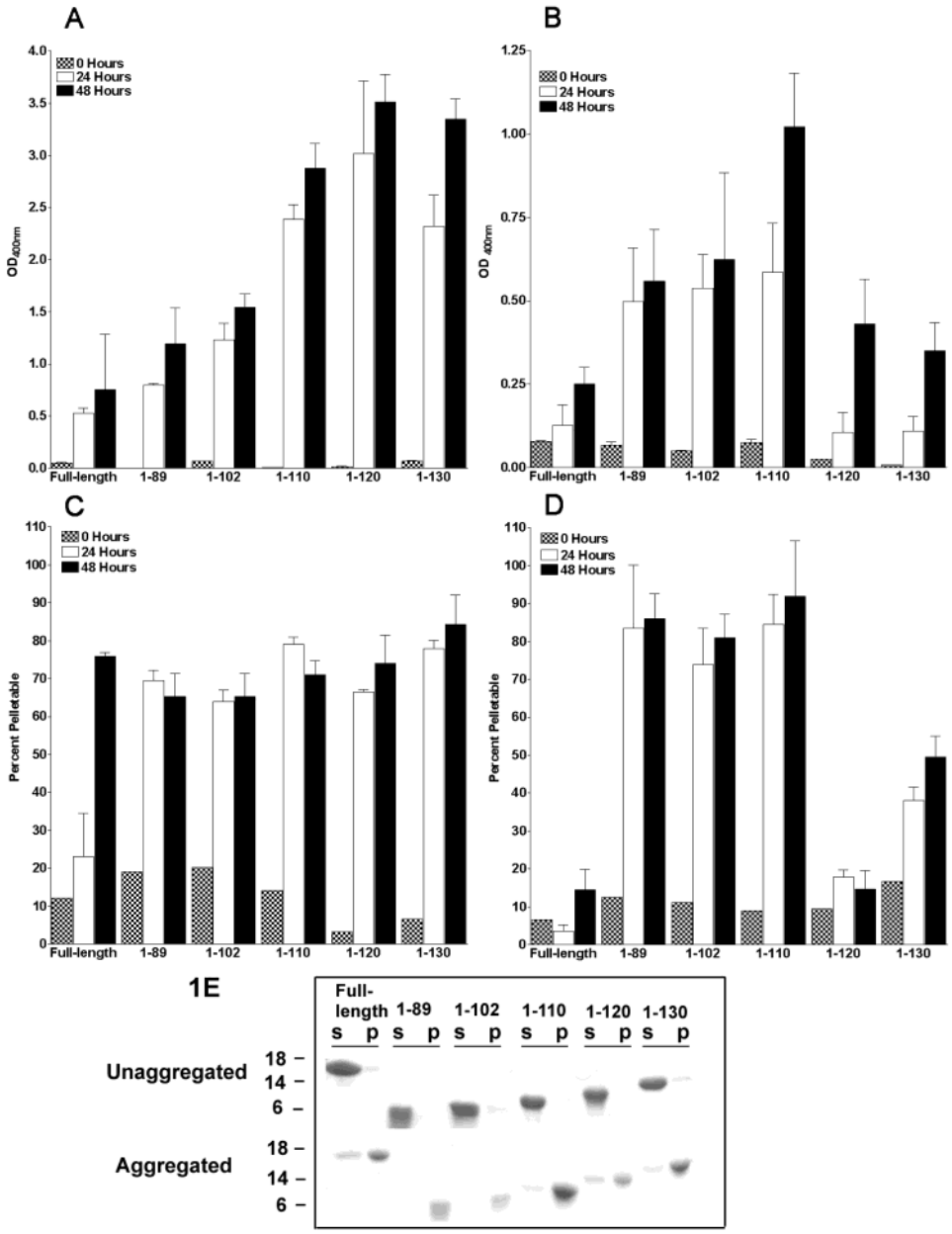

FIGURE 1: Comparison of the assembly efficiency of full-length and carboxy-terminal truncated α-syn. Each protein was incubated under assembly conditions (100 mM sodium acetate, pH 7.5) for 0, 24, and 48 h. Polymerization of α-syn proteins at 350 μM (A and C) and 100 μM (B and D) was assayed by turbidity OD_{400} (A and B) and sedimentation centrifugation analysis (C and D). $n = 4$ and error bars = sem. Representative Coomassie stained gels containing supernatants (s) and pellets (p) of aggregated and unaggregated proteins at equal protein concentrations (E).

which reached a maximum by 24 h (Figure 1D). By contrast, the longer proteins 1−120, 1−130, and full-length α-syn aggregate poorly at these concentrations, at both 24 and 48 h (Figure 1D). Thus, aggregation is affected by both truncation and concentration.

Carboxy-Terminal Truncated α-Syn Species Polymerize into β-Sheet Fibrils. To assess whether pelletable α-syn proteins formed ordered filaments with a β-sheet structure that is typical of all amyloid, or alternatively, unordered aggregates, we employed physical methods sensitive to polypeptide secondary structure, including CD spectroscopy (Figure 2A,B), ATR-FTIR spectroscopy (Figure 2C−E), and chemical dyes that detect amyloidogenic β-sheet conformation (e.g., K114 and ThioT) via fluorescence spectroscopy (Figure 2F,G).

The CD spectra for unaggregated α-syn proteins exhibited a minimum at 195−200 nm of molar ellipticity and a small negative shoulder at 215−230 nm, with a trend toward increasing intensity with an increasing length of the proteins (Figure 2A). The spectra indicate that α-syn is predominantly unstructured or random coil with a small amount of α-helix and β-sheet structure. Upon aggregation, all truncated and wild-type α-syn proteins showed some degree of β-sheet since the CD spectra showed a maximum at 200−205 and a negative deflection at 215−230 (Figure 2B), similar to previous observations (*28*). The less intense positive signal at 200−205 and the shift in the negative deflection from 230 to 215−220 nm with larger proteins suggest that the sample is a mixture of the spectra for unordered structure along with β-sheet structure. Significantly, 1−110 and 1−120

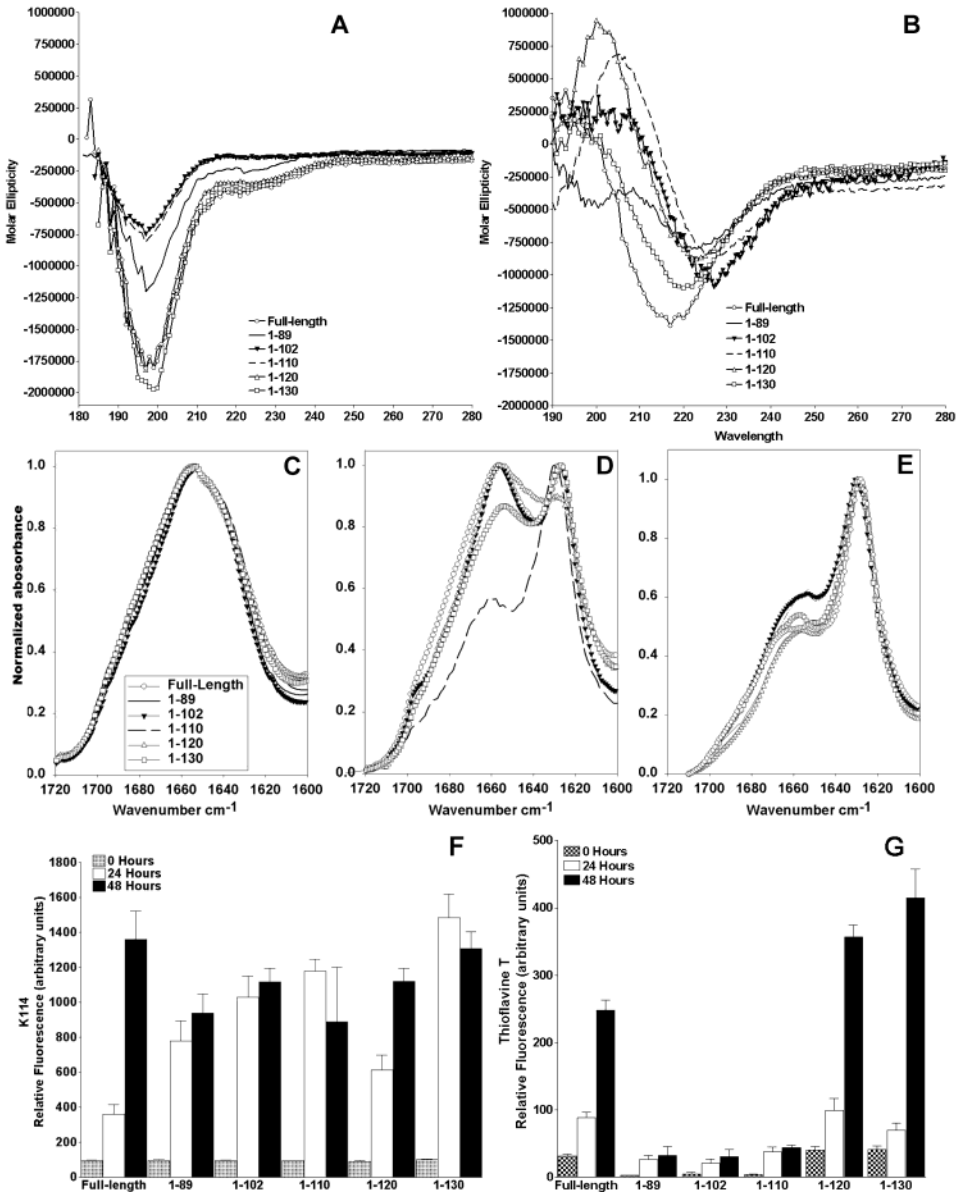

FIGURE 2: Formation of β-pleated sheet structure is associated with filament assembly of all truncated α-syn proteins. Circular dichroism of unassembled α-syn proteins (A) and 48-h assembled α-syn proteins (B) at 0.25 μg/μL in 300 μL of 100 mM phosphate buffer, pH 7.5, expressed as molar ellipticity. ATR-FTIR spectra in the amide I region of hydrated thin films of unassembled protein (C), assembled proteins with no centrifugation (D), and assembled proteins after centrifugation and resuspension of pelleted fibrils (E) were expressed as normalized absorbance. Protein samples consisted of 5 μL of 2 μg/μL α-syn in 10 mM HEPES in D_2O buffer at pH 7.4 dried onto a germanium internal reflection crystal. Fluorescence was measured on α-syn aggregated at 350 μM (F and G). K114 fluorescence of α-syn (F) and ThioT (G) in 100 mM sodium acetate buffer, pH 7.5, for 0, 24, and 48 h. Final protein concentrations were at 17.5 μM for K114 and 8.75 μM for ThioT fluorescence. $n = 4$ and error bars = sem.

but not the other α-syn variants adopted predominantly β-sheet structure since intense positive signals were detected at 200−205 nm.

The normalized ATR−FITR spectrum of unaggregated α-syn proteins demonstrated an absorption maximum at 1652−1660 cm^{-1} with a prominent shoulder at 1647 cm^{-1} consistent with the existence of non-β and unordered or random coil structures (Figure 2C). After aggregation, the peak at 1652−1660 cm^{-1} is prominent along with a peak at 1627 cm^{-1} and a small shoulder at 1695 cm^{-1} (Figure 2D) indicative of the presence of both unordered and β structure. Centrifugation to eliminate unaggregated α-syn and resuspension of the pellet to enrich for aggregated α-syn tended to reduce the contribution of the 1652−1656 cm^{-1} peak (Figure 2E) suggesting that during α-syn assembly, the proteins are converted from mostly unordered to predominantly β structure. Furthermore, it was noted that slower drying, air-drying, of the unaggregated α-syn resulted in a peak at 1627 cm^{-1}, indicating the presence of some β-sheet (data not shown).

Using a Congo red fluorescent derivative K114 to quantify the amount of amyloid formation, all of the α-syn preparations showed intense fluorescence particularly after 48 h of incubation (Figure 2F). The fluorescence for full-length and 1−120 α-syn showed marked increases over 24 and 48 h, with the other truncations (1−89, 1−102, 1−110, and 1−130) showing less changes with time (Figure 2F). By contrast, only α-syn fibrils formed from full-length, 1−120, and 1−130 but not the shorter carboxy-truncated proteins (i.e., 1−89, 1−102, and 1−110) showed appreciable ThioT

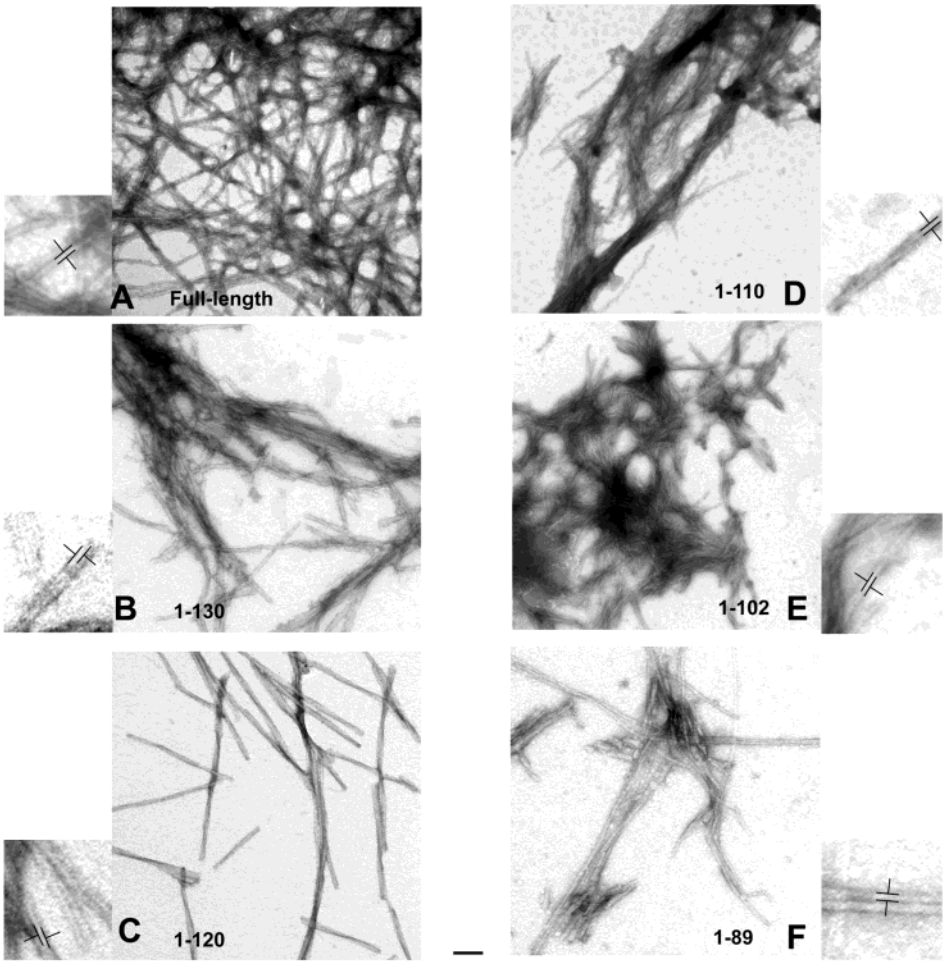

FIGURE 3: All α-syn proteins have a fibrillar ultrastructure. After aggregation in 100 mM sodium acetate, pH 7.5, for 48 h, samples of α-syn proteins were applied onto copper carbon coated grids and visualized by negative staining transmission EM with 1% aqueous uranyl acetate. Representative fields on the grids are depicted. The proteins and widths (nm) are full-length α-syn 10.54 ± 1.82 (A); 1−130, 6.76 ± 1.38 (B); 1−120, 8.73 ± 2.09 (C); 1−110, 6.71 ± 1.10 (D); 1−102, 8.17 ± 1.15 (E); and 1−89, 7.06 ± 1.47 (F). The widths represent the mean of 100−120 measurements of several fibers for each protein using Image-Pro Software. Magnification 120 000× and scale bar = 100 nm. The adjacent inserts for each panel are 4× software magnification of individual fibrils, demonstrating sample fibril widths. Some fibrils are seen as two or more strands (B, C, E, and F) and twisted strand pairs (D) (actual quantification of fibril widths listed above).

fluorescence particularly after 48 h of incubation (Figure 2G). The discrepancy between the intensity of fluorescence as detected by K114 versus ThioT for the larger C-terminus truncated 1−89, 1−102, and 1−110 is unknown at this time. However, it is well-known that not all *β*-sheet fibrils stain with ThioT (*45*, *46*), and it is possible that the removal of some of the negatively charged carboxy-terminal residues reduces the electrostatic interaction of the positively charged ThioT with α-syn.

Carboxy-Terminal Deletion Affects α-Syn Fibril Ultrastructure. To assess whether truncated α-syn proteins behave like the full-length protein and aggregate into 10 nm diameter fibrils, negative staining EM was performed. Figure 3A−F shows that all the aggregated α-syn proteins form unbranched fibrils, not amorphous aggregates, with the truncated α-syn species forming shorter fibrils that tended to bundle laterally. This is most notable for 1-110 (Figure 3D), which may explain the increased turbidity measurement (Figure 1B). Furthermore, the diameter of fibrils assembled from the carboxy-truncated α-syn proteins was less that of the full-length protein with widths for the different α-syn species as follows: full-length α-syn = 10.54 ± 1.82, 1−130 α-syn = 6.76 ± 1.38, 1−120 α-syn = 8.73 ± 2.09, 1−110 α-syn = 6.71 ± 1.10, 1−102 α-syn = 8.17 ± 1.15, and 1−89 α-syn = 7.06 ± 1.47 nm. This reduction in width of α-syn filaments upon truncation of the proteins suggested a role of the carboxy-terminus of α-syn in determining fibril widths. Moreover, 1−89, 1−102, and 1−130 formed long filaments that extended at least for several microns, similar to full-length α-syn (data not shown). Longer fibrils were occasionally observed for 1−120, but the majority of fibrils of 1−110 and 1−120 species were short (Figure 3C,D). Thus, all of the α-syn proteins studied here formed ordered fibrils, with slightly reduced widths upon carboxy-terminal truncation of α-syn.

NAC (61−95) Is Required for ANS Binding and Proteinase K Protection. The decreases in fibril widths upon α-syn carboxy-terminal truncation suggest differences in the fibril structure of the different species of α-syn. ANS binding, a hydrophobic binding dye, and proteinase K digestion were used to probe for structural differences. There was little ANS binding to the unaggregated α-syn proteins, with an increase in ANS fluorescence upon α-syn aggregation. Full-length and 1−130 species had little ANS binding at 24 h, which increased after 48 h (Figure 4A). The shorter α-syn truncations (i.e., 1−102 to 1−120) had biphasic ANS binding, with

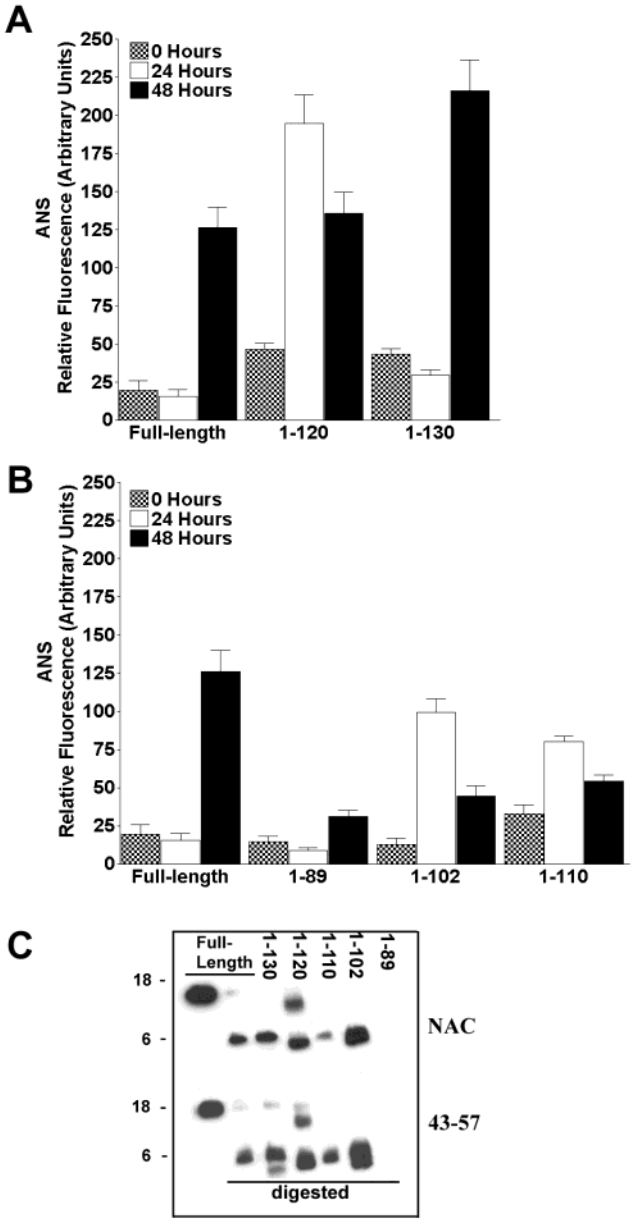

FIGURE 4: Complete NAC region (61−95) of α-syn involved in ANS fluorescence and proteinase K resistance. ANS fluorescence of α-syn proteins aggregated under assembly conditions for 0, 24, and 48 h at 350 μM (A) or 100 μM (B) was measured using 8.75 μM α-syn. $n = 4$, error bars = sem. Western analysis of 30 min proteinase K digestion of full-length and truncated α-syns after aggregation for 48 h and full-length undigested α-syn control, blotted with affinity purified NAC (75−91 epitope) and 43−57 α-syn polyclonal antibodies at 1:500 dilution (C).

increased binding at 24 h but then decreasing at 48 h (Figure 4B), which may be due to rearrangement of the fibrils over time resulting in less hydrophobic exposure. Notably, with deletion into the NAC region of α-syn, there was a reduction in solvent-exposed, hydrophobic ANS binding patches, especially for aggregated 1−89 (Figure 4B).

Protease K digestion of fibrillar α-syn proteins (from 1−102 through to full-length α-syn) resulted in the generation of similar molecular weight protease resistant fragments (Figure 4C). These fragments were mapped to the 43−95 amino acid region of α-syn using epitope specific antibodies (Figure 4C). Interestingly, α-syn 1−89, which showed little ANS binding (Figure 4B), also showed little protease resistance (Figure 4C). Thus, the entire NAC region partakes in formation of the secondary structure required to generate both ANS binding and protease K resistance.

Reduced Antibody Binding to Centrally Located α-Syn Epitopes. The differences in fiber widths, protease resistance, and ANS binding of the α-syn truncations prompted us to utilize immuno-EM to probe ultrastructural differences in the different α-syn species. In general, the epitope exposure within the α-syn fibrils is as follows: amino-terminal (amino acids 2−12) > carboxy-terminal > NAC region. The 2−12 amino acid epitope, as detected with amino terminal epitope specific antibodies Syn 505 and SNL-4, is regularly distributed along the length of the fibril for all of the α-syn proteins (Figure 5A−D). However, the immunostaining of the central region of α-syn mapping to 43−57 (Syn 43−57) (Figure 5F) and 75−91 (NAC) (Figure 5H) was reduced for full-length α-syn, suggesting some degree of epitope masking or sequestration within the α-syn fibril. Deletion within the NAC region of α-syn, in 1−89, appeared to increase exposure of the NAC epitope (Figure 5G) but not that of Syn 43−57 (Figure 5E). Finally, the carboxy-terminal regions of α-syn such as 89−110 (detected by Syn 204) and 104−119 (detected by SNL1) were exposed (Figure 5I−K and L, respectively) with no immunostaining of α-syn fibrils upon omission of the primary antibody (Figure 5M). Thus, there is some sequestering of the central region within the fibril, as evidenced by protease K digestion, and this region becomes more exposed upon partial deletion of the NAC.

Co-Assembly of Full-Length and Truncated α-Syn. Since there were reduced epitope exposures of the carboxy and predominantly the NAC regions, the truncations may have differing effects in seeding unaggregated full-length α-syn. For these experiments, α-syn protein at a total concentration of 200 μM were incubated under assembly conditions for 1 day shaking at 37 °C. Under these conditions, full-length α-syn and 1−130 incubated alone were predominantly unassembled (Figure 6C). Thus, seeding by the unaggregated truncations on full-length α-syn could be easily observed. The truncations 1−89 through 1−120 alone were able to aggregate at 200 μM after 1 day shaking at 37 °C (Figure 6A,C). For seeding of the full-length α-syn, molar ratios of 5:1, 1:1, and 1:5 for unaggregated, truncated α-syn to full-length α-syn were used (total protein concentration 200 μM). 1−120 was unable to seed at any concentration (Figure 6A) consistent with its inability to aggregate at 100 μM after 24 h (Figure 1B,D). By contrast, α-syn 1−89 through 1−110 were seeding competent, leading to greater turbidity (Figure 6A) as well as an increase in the amount of full-length α-syn in the pelleted fraction (Figure 6C). However, 1−89 was less efficient in seeding than 1−102 and 1−110 since these longer α-syn truncated proteins were capable of seeding at all concentrations tested (i.e., 150, 100, and 50 μM) thereby implicating the complete NAC region in α-syn aggregation (Figure 6A,C). These results indicate that the carboxyl region reduces the aggregation propensity, in which the region between 102 and 120 appears to be most important.

Mutation of Carboxy-Terminal Charged Residues in α-Syn. Some notable features of the α-syn sequence between residues 100 and 120 (^{101}GKNEEGAPQE^{110} GILED-MPVDP^{120}) are several prolines (residues P108, P117, and P120) as well as two pairs of negatively charged amino acids (residues E104/E105 and E114/D115). Since a lowered pH

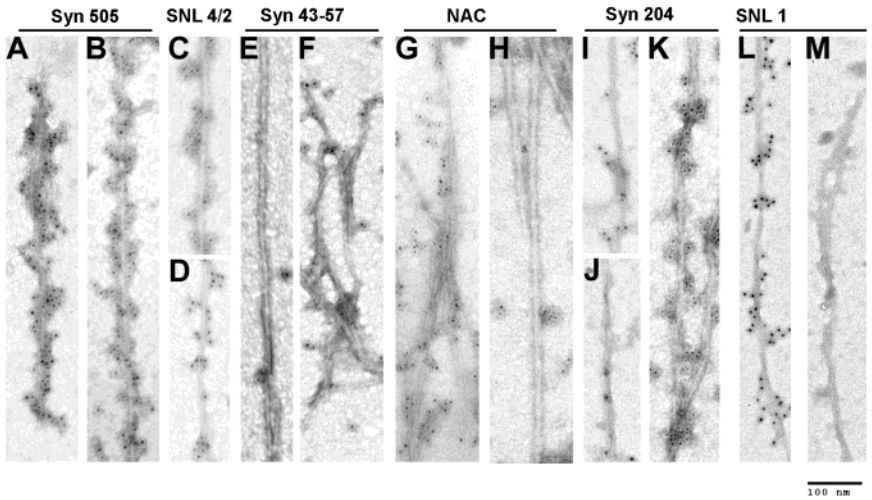

FIGURE 5: Central epitopes of α-syn proteins are masked by immunoelectron microscopy. After incubation in 100 mM sodium acetate, pH 7.5, for 48 h, samples of α-syn proteins were applied onto copper carbon coated grids and visualized by negative staining transmission EM with 1% aqueous uranyl acetate. The primary antibodies were used at 1:200 and the secondary 5 nm colloidal gold conjugated antibody at 1:20 dilutions. Antibody Syn 505 (epitope 2−12) was used on α-syn 1−89 (A) and 1−110 (B). SNL-4 (with the same epitope 2−12) is shown with proteins 1−120 (C) and full-length α-syn (D). Syn 43−57 and NAC (epitope 75−91) immunolabeling are shown for the representative proteins 1−89 (E and G) and full-length α-syn (F and H), respectively. Syn 204 (epitope 89−110) immunolabeling for 1−110, 1−120, and full-length are demonstrated in panels I, J, and K, while SNL1 (epitope 104−119) for full-length is demonstrated in panel L. Full-length α-syn is shown with the control secondary antibody alone in (M). Magnification 120 000× and scale bar = 100 nm.

resulted in increased α-syn aggregation (*15*, *29*), charged amino acids and not prolines are more likely to be responsible for mediating this effect. Thus, pairs of negatively charged amino acids E104, E105 and E114, D115 were mutated to alanines in the 1−120 α-syn protein. While 1−120 was unable to aggregate at 100 μM, mutating the residues E104A−E105A and E114A−D115A enabled aggregation at this concentration (data not shown). Significantly, mutations of these pairs of charges also rendered the proteins seeding permissive (Figure 6B,D).

DISCUSSION

Utilizing several different complementary assays and a variety of wild-type and mutant or truncated α-syn constructs, we have dissected out the relative contributory role of the central NAC and carboxy regions of α-syn in fibril formation. Specifically, we confirm and extend earlier data showing that the NAC region forms the hydrophobic, protease resistant core of α-syn fibrils and show for the first time that the carboxy-terminus of α-syn and negative charges within this domain exert countervailing influences on α-syn fibrillization at the initial steps of polymerization and seeding.

Comparison of the different techniques used for assaying fibril formation highlighted the drawbacks of some of the techniques, of which a few will be discussed. Centrifugal sedimentation rather than turbidity was more accurate in determining aggregation, especially at lower α-syn concentrations. Turbidity, while a rapid nondestructive technique, is affected by factors such as fibril widths/clumping and sedimentation of the fibrils. Because both of these techniques cannot differentiate between amorphous aggregates and fibrils, other methods such as CD, FTIR, or β-sheet binding dyes that determine β-sheet secondary structure or EM that detect fibril morphology are required to document the presence of α-syn amyloid fibrils. However, caution must be exercised in interpreting some of the data. For example, ThioT has been used to measure β-sheet structure, but not all β-sheet fibrils stain with ThioT. In our study, ThioT binds very poorly to fibrillar 1−89, 1−102, and 1−110 α-syn protein similar to other polypeptides such as poly(L-serine) or poly(L-lysine) (*45*) and truncated forms of amylin (*45*, *46*). For α-syn, this reduced ThioT binding may be due to clumping of fibrils obscuring the ThioT binding sites, a mechanism similar to those previously reported (*47*). Also, since there is a pH dependence of ThioT binding to amyloid (*45*, *48*, *49*), this suggests that the interaction may be electrostatic. Thus, the removal of the negatively charged, carboxy-terminal of α-syn may reduce its interaction with the positively charged ThioT. This problem was overcome when we used K114, a fluorescent congener of Congo red, X-34, and BSB (*43*, *44*). Our recent studies suggest that K114 provides a more quantitative measurement of β-sheet fibrils formed from α-syn, tau, and the amyloid β-peptide (*59*). Finally, CD and FTIR are particularly robust methods of assaying secondary structure, with EM of the aggregates being most definitive for the presence of fibrils.

The physical assays, turbidity measurements, and sedimentation experiments indicated that the carboxy-terminal truncated α-syn species aggregated more rapidly, and at lower concentrations, than full-length α-syn. To understand the reasons for this, we characterized the secondary structure and ultrastructure of full-length and truncated α-syn. Notably, all of the proteins analyzed here, including 1−89 formed β-sheet structures upon aggregation. Similar structural changes between unaggregated (*28*, *50*) and aggregated α-syns were observed in the circular dichroism obtained here as previously published reports for 1−87, 1−120 truncations, and full-length α-syns (*28*), but ATR-FTIR detected both non-β-sheet and β-sheet structures in aggregated samples, and it did so with much smaller samples than circular dichroism (5 vs 150 μg). Since 1−89 is competent for fibril formation, this indicates that NAC and the amino-terminal

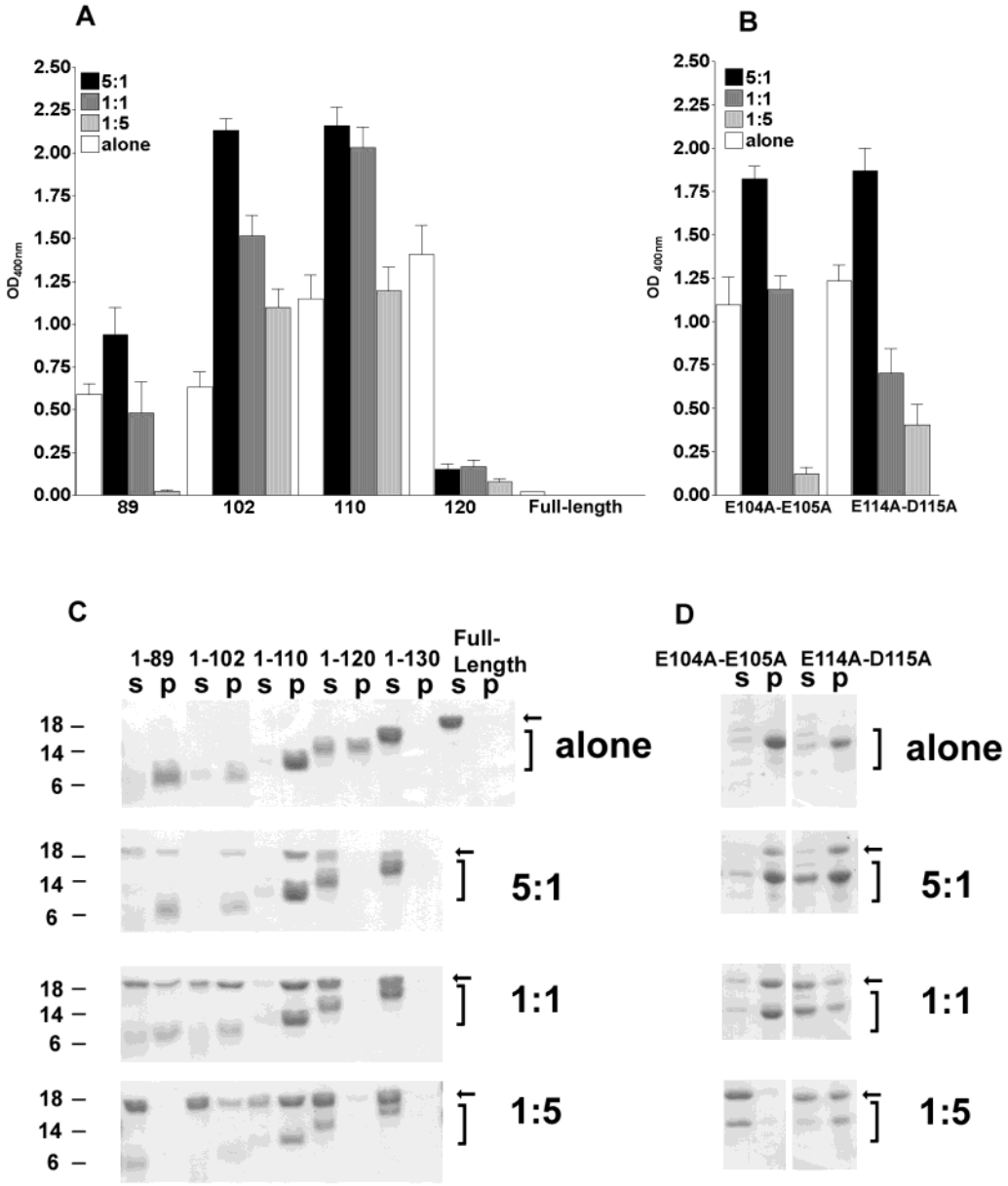

FIGURE 6: Co-assembly of full-length α-syn with carboxy-terminal truncated protein. The α-syn truncations and additional point mutations in 1−120 (E104A−E105A and E114A−D115A) were incubated alone or with truncated and full-length α-syn proteins at ratios of 5:1, 1:1, or 1:5, respectively (200 μM total), aggregated for 24 h in 100 mM sodium acetate, pH 7.5. Aggregation was analyzed by turbidity (A and B) and centrifugal sedimentation (C and D). Arrows indicate full-length protein, and square brackets depict truncated proteins. S and P represent supernatants and pellets, respectively.

region but not the carboxy-terminus of α-syn are required for fibril formation. This observation is consistent with the amino-terminal A53T mutant aggregating more rapidly (*16*, *26*, *36*) as well as a recent study involving amino terminal repeat deletions (*39*) and the NAC region being essential for polymerization (*23*).

Since the truncated species of α-syn appeared shorter and bundled laterally, as noted previously (*28*), reductions in fibrils widths, along with the immuno-EM data, suggest that the carboxy-terminus of α-syn is peripheral to the α-syn fibril. However, we noted that the fiber widths did not track precisely with the extent of truncation, and specific residues may play a role in this packing mechanism since 1−120 with a terminal proline is the outlier with a wider diameter than the other truncation mutants. Reductions of widths were also noted upon proteinase K removal of the amino and carboxyl regions (*51*). Epitope mapping of the fibrils indicated that the NAC is buried within fibrils and that the carboxy- and amino-termini are exposed and the NAC region (i.e., amino acids 75−91) is sequestered within the α-syn fibril where it may be involved in forming the fibril core. This is supported by the fact that disruption of the NAC region reduced ANS binding and abolished proteinase K protection as well as data from other recent studies where antibody binding to the NAC increased after protease digestion (*51*).

From the seeding experiments, regions modulating aggregation were identified, including the NAC region and negatively charged carboxy-terminus of α-syn. The hydrophobic NAC region has previously been implicated in α-syn fibrillization (*23*, *24*, *37*, *38*), and the NAC region appears to be essential for seeding based on our studies of deletions within the NAC region that reduced the seeding ability of the 1−89 α-syn species. In contrast, the carboxy-terminus of α-syn appears to be partially inhibitory to α-syn aggrega-

tion, as suggested previously (*28*), and we show here that decreasing the carboxy-terminal lengths of α-syn increased the aggregation and efficiency of seeding of α-syn (Figures 1 and 6). This is consistent with the notion that α-syn has a chaperone function (*50*, *52*) as well as with data showing that the carboxy-terminal domain of α-syn fused with GST prevented denaturation of α-syn (*53*). This chaperone activity of α-syn on proteins was mapped to the second acidic repeat of α-syn using synthetic peptides (*50*). We focused our attention on the residues before 120 for the following reasons. Increased α-syn aggregation because of truncation exhibited dramatic dichotomy at lower α-syn concentrations, with 1−120 being incompetent and 1−102 and 1−110 both being especially competent for aggregation (100 μM at 24 h, Figure 1B). Furthermore, both the truncations 1−102 and 1−110 overcame the inhibitory effect of full-length α-synuclein on fibrillogenesis, while 1−120 did not (Figure 6A,C). Thus, the region below 120 residues, especially the paired negative charges, was studied further. Our present study also demonstrated a novel inhibitory region in the carboxy-terminus of α-syn, which appeared to play a role in inhibiting its own aggregation. We identified negatively charged amino acids at 104, 105 and 114, 115 in the carboxy-terminus of α-syn to be responsible for this inhibitory activity in 1−120.

It is plausible that the negative charges in the last 20 amino acids of α-syn can contribute to the chaperone effect in light of the present data. Electrostatic interactions appear to be involved in the chaperone activity and aggregation, as sodium chloride reduced the chaperone effect of α-syn on aldolase (*50*) and accelerated the aggregation of full-length α-syn (*54*). However, retardation of α-syn aggregation may be a different process than that of chaperoning, and further studies are required. For example, it is possible that aggregation is inhibited by the extended nature of the carboxy-terminal, stiffness/inflexibility around residues 122 (*55*), or a postulated interaction of the carboxy-terminal with the NAC region (*56*).

Although the normal function and biological properties of different domains of α-syn remain to be elucidated, pathological truncation of α-syn may result in an increased propensity of α-syn to aggregate in the brains of patients destined to develop a neurodegenerative synucleinopathy. However, while truncated fragments of α-syn may occur in MSA brains (*57*), α-syn fragments appear not to be specific to pathology in synucleinopathies (*58*). If 1−120 is formed in vivo, as may occur in vitro (*26*), extrapolation from our data would indicate that it is unlikely to be pathogenic since it cannot readily seed full-length α-syn. Alternatively, any truncation of α-syn to form fragments of 1−102 or 1−110 could be more detrimental to the human brain. However, these in vitro experiments notwithstanding, other in vivo factors (e.g., lipid binding, other posttranslational modifications, etc.) likely contribute to the pathogenic role of α-syn in human disease brains, and animal models may be most suited to elucidating these questions. Nonetheless, a more concise understanding of the fibril morphology and aggregation mechanism of α-syn proteins is emerging, and this will accelerate development of compounds that can inhibit α-syn aggregation and perhaps be used therapeutically to intervene in neurodegenerative synucleinopathies.

ACKNOWLEDGMENT

The authors thank Drs. K. S. Reddy and C. Moser of the Johnson Research Foundation for assistance with circular dichroism and Neelema Shah of the Biochemical Imaging Core Facility of the University of Pennsylvania for assistance with the electron microscopy. We also thank Linda Kwong for her insightful discussions.

REFERENCES

1. Spillantini, M. G., Schmidt, M. L., Lee, V. M.-Y., Trojanowski, J. Q., Jakes, R., and Goedert, M. (1997) *Nature 388*, 839−840.
2. Baba, M., Nakajo, S., Tu, P. H., Tomita, T., Nakaya, K., Lee, V. M.-Y., Trojanowski, J. Q., and Iwatsubo, T. (1998) *Am. J. Pathol. 152*, 879−884.
3. Wakabayashi, K., Matsumoto, K., Takayama, K., Yoshimoto, M., and Takahashi, H. (1997) *Neurosci. Lett. 239*, 45−48.
4. Kruger, R., Kuhn, W., Muller, T., Woitalla, D., Graeber, M., Kosel, S., Przuntek, H., Epplen, J. T., Schols, L., and Riess, O. (1998) *Nat. Genet. 18*, 106−108.
5. Polymeropoulos, M. H., Lavedan, C., Leroy, E., Ide, S. E., Dehejia, A., Dutra, A., Pike, B., Root, H., Rubenstein, J., Boyer, R., Stenroos, E. S., Chandrasekharappa, S., Athanassiadou, A., Papapetropoulos, T., Johnson, W. G., Lazzarini, A. M., Duvoisin, R. C., Di Iorio, G., Golbe, L. I., and Nussbaum, R. L. (1997) *Science 276*, 2045−2047.
6. Masliah, E., Rockenstein, E., Veinbergs, I., Mallory, M., Hashimoto, M., Takeda, A., Sagara, Y., Sisk, A., and Mucke, L. (2000) *Science 287*, 1265−1269.
7. Feany, M. B., and Bender, W. W. (2000) *Nature 404*, 394−398.
8. Auluck, P. K., Chan, H. Y., Trojanowski, J. Q., Lee, V. M.-Y., and Bonini, N. M. (2002) *Science 295*, 865−868.
9. Giasson, B., Duda, J. E., Quinn, S. M., Zhang, B., Trojanowski, J. Q., and Lee, V. M.-Y. (2002) *Neuron 34*, 521−533.
10. Lee, M. K., Stirling, W., Xu, Y., Xu, X., Qui, D., Mandir, A. S., Dawson, T. M., Copeland, N. G., Jenkins, N. A., and Price, D. L. (2002) *Proc. Natl. Acad. Sci. U.S.A. 99*, 8968−8973.
11. Tu, P. H., Galvin, J. E., Baba, M., Giasson, B., Tomita, T., Leight, S., Nakajo, S., Iwatsubo, T., Trojanowski, J. Q., and Lee, V. M.-Y. (1998) *Ann. Neurol. 44*, 415−422.
12. Spillantini, M. G., Crowther, R. A., Jakes, R., Cairns, N. J., Lantos, P. L., and Goedert, M. (1998) *Neurosci. Lett. 251*, 205−208.
13. Arawaka, S., Saito, Y., Murayama, S., and Mori, H. (1998) *Neurology 51*, 887−889.
14. Conway, K. A., Harper, J. D., and Lansbury, P. T. (1998) *Nat. Med. 4*, 1318−1320.
15. Hashimoto, M., Hsu, L. J., Sisk, A., Xia, Y., Takeda, A., Sundsmo, M., and Masliah, E. (1998) *Brain Res. 799*, 301−306.
16. Giasson, B. I., Uryu, K., Trojanowski, J. Q., and Lee, V. M.-Y. (1999) *J. Biol. Chem. 274*, 7619−7622.
17. Narhi, L., Wood, S. J., Steavenson, S., Jiang, Y., Wu, G. M., Anafi, D., Kaufman, S. A., Martin, F., Sitney, K., Denis, P., Louis, J. C., Wypych, J., Biere, A. L., and Citron, M. (1999) *J. Biol. Chem. 274*, 9843−9846.
18. El Agnaf, O. M., Jakes, R., Curran, M. D., and Wallace, A. (1998) *FEBS Lett. 440*, 67−70.
19. Arima, K., Ueda, K., Sunohara, N., Hirai, S., Izumiyama, Y., Tonozuka-Uehara, H., and Kawai, M. (1998) *Brain Res. 808*, 93−100.
20. Arima, K., Ueda, K., Sunohara, N., Arakawa, K., Hirai, S., Nakamura, M., Tonozuka-Uehara, H., and Kawai, M. (1998) *Acta Neuropathol. (Berlin) 96*, 439−444.
21. Spillantini, M. G., Crowther, R. A., Jakes, R., Hasegawa, M., and Goedert, M. (1998) *Proc. Natl. Acad. Sci. U.S.A. 95*, 6469−6473.
22. Crowther, R. A., Daniel, S. E., and Goedert, M. (2000) *Neurosci. Lett. 292*, 128−130.
23. Giasson, B. I., Murray, I. V., Trojanowski, J. Q., and Lee, V. M.-Y. (2001) *J. Biol. Chem. 276*, 2380−2386.
24. Biere, A. L., Wood, S. J., Wypych, J., Steavenson, S., Jiang, Y., Anafi, D., Jacobsen, F. W., Jarosinski, M. A., Wu, G. M., Louis, J. C., Martin, F., Narhi, L. O., and Citron, M. (2000) *J. Biol. Chem. 275*, 34574−34579.
25. Wood, S. J., Wypych, J., Steavenson, S., Louis, J. C., Citron, M., and Biere, A. L. (1999) *J. Biol. Chem. 274*, 19509−19512.
26. Conway, K. A., Harper, J. D., and Lansbury, P. T., Jr. (2000) *Biochemistry 39*, 2552−2563.

27. Conway, K. A., Lee, S. J., Rochet, J. C., Ding, T. T., Williamson, R. E., and Lansbury, P. T., Jr. (2000) *Proc. Natl. Acad. Sci. U.S.A. 97*, 571−576.
28. Serpell, L. C., Berriman, J., Jakes, R., Goedert, M., and Crowther, R. A. (2000) *Proc. Natl. Acad. Sci. U.S.A. 97*, 4897−4902.
29. Uversky, V. N., Li, J., and Fink, A. L. (2001) *J. Biol. Chem. 276*, 10737−10744.
30. Han, H., Weinreb, P. H., and Lansbury, P. T., Jr. (1995) *Chem. Biol. 2*, 163−169.
31. Uversky, V. N., Li, J., and Fink, A. L. (2001) *FEBS Lett. 500*, 105−108.
32. Uversky, V. N., Li, J., and Fink, A. L. (2001) *J. Biol. Chem. 276*, 44284−44296.
33. Uversky, V. N., Lee, H. J., Li, J., Fink, A. L., and Lee, S. J. (2001) *J. Biol. Chem. 276*, 43495−43498.
34. Uversky, V. N., Li, J., Souillac, P., Jakes, R., Goedert, M., and Fink, A. L. (2002) *J. Biol. Chem. 277*, 11970−11978.
35. Cohlberg, J. A., Li, J., Uversky, V. N., and Fink, A. L. (2002) *Biochemistry 41*, 1502−1511.
36. Li, J., Uversky, V. N., and Fink, A. L. (2001) *Biochemistry 40*, 11604−11613.
37. Hashimoto, M., Rockenstein, E., Mante, M., Mallory, M., and Masliah, E. (2001) *Neuron 32*, 213−223.
38. Kahle, P. J., Neumann, M., Ozmen, L., Muller, V., Odoy, S., Okamoto, N., Jacobsen, H., Iwatsubo, T., Trojanowski, J. Q., Takahashi, H., Wakabayashi, K., Bogdanovic, N., Riederer, P., Kretzschmar, H. A., and Haass, C. (2001) *Am. J. Pathol. 159*, 2215−2225.
39. Kessler, J. C., Rochet, J. C., and Lansbury, P. T., Jr. (2003) *Biochemistry 42*, 672−678.
40. Crowther, R. A., Jakes, R., Spillantini, M. G., and Goedert, M. (1998) *FEBS Lett. 436*, 309−312.
41. Giasson, B. I., Jakes, R., Goedert, M., Duda, J. E., Leight, S., Trojanowski, J. Q., and Lee, V. M.-Y. (2000) *J. Neurosci. Res. 59*, 528−533.
42. Duda, J. E., Giasson, B., Mabon, M. E., Lee, V. M.-Y., and Trojanowski, J. Q. (2002) *Ann. Neurol. 52*, 205−210.
43. Styren, S. D., Hamilton, R. L., Styren, G. C., and Klunk, W. E. (2000) *J. Histochem. Cytochem. 48*, 1223−1232.
44. Lee, C. W., Zhuang, Z. P., Kung, M. P., Plossl, K., Skovronsky, D., Gur, T., Hou, C., Trojanowski, J. Q., Lee, V. M., and Kung, H. F. (2001) *J. Med. Chem. 44*, 2270−2275.
45. LeVine, H., III (1999) *Methods Enzymol. 309*, 274−284.
46. Goldsbury, C., Goldie, K., Pellaud, J., Seelig, J., Frey, P., Muller, S. A., Kistler, J., Cooper, G. J., and Aebi, U. (2000) *J. Struct. Biol. 130*, 352−362.
47. Souillac, P. O., Uversky, V. N., Millett, I. S., Khurana, R., Doniach, S., and Fink, A. L. (2002) *J. Biol. Chem. 277*, 12666−12679.
48. Naiki, H., Higuchi, K., Hosokawa, M., and Takeda, T. (1989) *Anal. Biochem. 177*, 244−249.
49. LeVine, H., III (1993) *Protein Sci. 2*, 404−410.
50. Kim, T. D., Paik, S. R., and Yang, C. H. (2002) *Biochemistry 41*, 13782−13790.
51. Miake, H., Mizusawa, H., Iwatsubo, T., and Hasegawa, M. (2002) *J. Biol. Chem. 277*, 19213−19219.
52. Kim, T. D., Paik, S. R., Yang, C. H., and Kim, J. (2000) *Protein Sci. 9*, 2489−2496.
53. Park, S. M., Jung, H. Y., Chung, K. C., Rhim, H., Park, J. H., and Kim, J. (2002) *Biochemistry 41*, 4137−4146.
54. Hoyer, W., Antony, T., Cherny, D., Heim, G., Jovin, T. M., and Subramaniam, V. (2002) *J. Mol. Biol. 322*, 383−393.
55. Bussell, R., Jr., and Eliezer, D. (2001) *J. Biol. Chem. 276*, 45996−46003.
56. McLean, P. J., and Hyman, B. T. (2002) *Neurosci. Lett. 323*, 219−223.
57. Gai, W. P., Power, J. H., Blumbergs, P. C., Culvenor, J. G., and Jensen, P. H. (1999) *J. Neurochem. 73*, 2093−2100.
58. Culvenor, J. G., McLean, C. A., Cutt, S., Campbell, B. C., Maher, F., Jakala, P., Hartmann, T., Beyreuther, K., Masters, C. L., and Li, Q. X. (1999) *Am. J. Pathol. 155*, 1173−1181.
59. Crystal, A. S., Giasson, B. I., Crowen, A., Kung, M.-P., Zhuang, Z.-P., Trojanowski, J. Q., and Lee, V. M.-Y. (2003) *J. Neurochem.*, in press.

BI027363R